Free Calcium Concentrations in Bullfrog Rods Determined in the Presence of Multiple Forms of Fura-2

Sean T. McCarthy, James P. Younger, and W. Geoffrey Owen
Neurobiology Division, Department of Molecular and Cell Biology, University of California, Berkeley, California 94720-3200 USA

ABSTRACT We employed the fluorescent calcium indicator Fura-2, loaded into intact retinas of the bullfrog *Rana catesbeiana*, to measure free calcium concentrations in the rod outer-segment cytosol. We determined that traditional methods of calculation yielded erroneous values of calcium. This error results from the presence of at least two distinct pools of Fura-2 in rod outer segments. Application of manganese quenches each pool, but quenching occurs at different rates. Using this fact, we show that the pools can be isolated by brief exposure to manganese and examined separately. One of these pools has the same fluorescent properties as the free salt of Fura-2 we use in our in vitro calibrations. The other source of fluorescence has more unusual properties. Although insensitive to calcium concentrations in the physiological range, it contributes significant anomalous fluorescence when cytosolic free calcium concentrations are elevated by application of IBMX. Nevertheless, the experimentally isolated, classic pool of Fura-2 is well behaved and allows us to calculate calcium concentrations relative to the K_d of Fura-2 by the usual ratio method. We show that when rods are exposed to saturating light, the free calcium concentration in their outer segments falls to a level not significantly different from zero within 20–30 s.

INTRODUCTION

Cytosolic free calcium ($[Ca^{2+}]_i$) has been cast with an important role in the story of phototransduction (see, for example, Pugh and Altman, 1988). It is involved in regulating the change in sensitivity of photoreceptors, which is the hallmark of light adaptation. Two observations have made this evident. First, when the rate of change of free calcium is slowed by incorporating a high concentration of the calcium buffer BAPTA (1,2-bis(*o*-aminophenoxy)ethane-*N*,*N*,*N*′,*N*′-tetraacetic acid) into rods, the recovery of the photocurrent from illumination is slowed dramatically (Torre et al., 1986). Second, bathing a photoreceptor in a medium that minimizes light-induced changes in $[Ca^{2+}]_i$ abolishes the principal features of light adaptation (Matthews et al., 1988; Nakatani and Yau, 1988). It was to understand more clearly its part in light adaptation that we attempted to measure $[Ca^{2+}]_i$ in rod outer segments both in the dark and in response to illumination.

Biochemical and electrophysiological experiments have suggested more than one way in which calcium might exert an adaptive influence on phototransduction. Varying cytosolic free calcium concentration between 30 nM and 1 μM reportedly affects the light-activated cascade that leads to the closure of cyclic GMP-gated channels in the rod outer-segment plasma membrane (Bownds, 1980; Robinson et al., 1980; Wagner et al., 1989; Kawamura and Murakami, 1991; Kawamura, 1993; McCarthy, 1993; Pepperberg et al., 1994; Lagnado and Baylor, 1994.). Additionally, a series of reports (Lolley and Racz, 1982; Pepe et al., 1986; Koch and Stryer, 1988; Dizhoor et al., 1991) has attributed modulation of the activity of guanylate cyclase to $[Ca^{2+}]_i$ in the range around or below 100 nM. This enzyme controls the production of cyclic GMP and, thus, probably plays a part in the recovery of rods from illumination. To assess whether these effects occur in intact photoreceptors and, if they do, what their relative importance might be requires a reliable description of light-induced changes in $[Ca^{2+}]_i$.

Earlier attempts to measure cytosolic free calcium failed to produce a definitive result. A light-induced fall in cytosolic calcium was inferred from the activity of an electrogenic ion-exchange mechanism that continued to extrude calcium in exchange for extracellular sodium after all outer-segment channels had been closed by light (Yau and Nakatani, 1985; Hodgkin et al., 1985; Miller and Korenbrot, 1987). An effort to determine $[Ca^{2+}]_i$ directly, using the photoprotein aequorin in salamander rods, yielded an upper limit in the dark of 0.6 μM (McNaughton et al., 1986). More recent work with the same technique resulted in an estimate for $[Ca^{2+}]_i$ of 0.4 μM in the dark (Lagnado et al. 1992), falling to an undetectable level below 0.3 μM in saturating light. Using the more sensitive calcium probe Quin2, Korenbrot and Miller (1989) measured cytosolic free calcium concentration in toad rods to be 273 ± 129 nM in the dark and not less than 50 nM in bright light. Previous work in our laboratory (Ratto et al., 1988), using the fluorescent dye Fura-2, yielded values of 220 nM in the dark and about 140 nM after 6 s of saturating illumination.

Taken at face value, these findings suggest that $[Ca^{2+}]_i$ does not change over the full range thought to modulate intracellular enzymes. A more serious challenge to the concentrations reported during bright illumination comes from the work of Cervetto et al. (1989) and Schnetkamp et al. (1989), which demonstrated that potassium is extruded along with calcium by the exchange mechanism. During bright illumination, when all cyclic GMP-gated channels are shut (Baylor and Nunn, 1986), the Na^+:Ca^{2+}, K^+ exchanger is

Received for publication 24 November 1994 and in final form 10 June 1994.
Address reprint requests to Dr. W. Geoffrey Owen, Dept. of Molecular & Cell Biology, Univ. of California, Berkeley, Life Sciences Addition, Box 181, Berkeley, CA 94720-3200. Tel.: 510-643-8878; Fax: 510-642-9933.

0006-3495/94/11/2076/14 $2.00

expected to reach equilibrium. If that were the case, the cytosolic free calcium concentration should be less than 1 nM at this point, well below the values indicated by the earlier studies.

It has been suggested, however, that the Na^+:Ca^{2+}, K^+ exchanger inactivates before equilibrium is reached (Schnetkamp et al., 1991; Schnetkamp and Szerencsei, 1993) and, thus, the cytosolic free calcium concentration remains above its equilibrium value. In this paper, we present strong evidence that the apparently nonzero value of calcium measured by Fura-2 in saturating light does correspond to $[Ca^{2+}]_i \approx 0$ as would be expected if the exchanger reached equilibrium. When a retina is perfused for a prolonged period with a solution that contains no free calcium to reduce cytosolic free calcium to a very low level, the apparent $[Ca^{2+}]_i$ indicated by Fura-2 is not different from that measured after bright light. We will show in this paper that the discrepancy is caused by a failure of Fura-2 to act the same way in rod cells as it does in vitro. Specifically, we show that at least two distinct pools of Fura-2 exist in the outer segment. One of these pools, which is the only pool that responds to physiological, light-induced changes in calcium, has properties nearly identical to the free salt of Fura-2 that we use in our in vitro calibrations. We show that when we isolate this pool experimentally, the cytosolic free calcium concentrations we calculate both during saturating illumination and during exposure to the calcium-free perfusate are not significantly different from zero. As important, the properties of the experimentally isolated pool of Fura-2 allow us to describe with confidence the time course of changes in free calcium induced by light, a prerequisite to a complete understanding of phototransduction. (Preliminary results were reported by Younger (1991), Younger et al. (1992), and McCarthy (1993).)

MATERIALS AND METHODS

Dissection

Retinas were obtained from large bullfrogs, *Rana catesbeiana*. Frogs were killed by decapitation and double-pithed in dim red light after overnight dark adaptation. Eyes were enucleated, and all remaining procedures were carried out under infrared illumination using an image converter or in the dark. Retinal halves were prepared and placed separately into vials containing 2 ml of the control solution described below supplemented with 12.5 μM acetoxymethyl ester of Fura-2 (Fura-2 AM), 0.015% Pluronic F-127 (both supplied by Molecular Probes, Eugene, OR), and 1.9% fetal calf serum (Sigma Chemical Co., St. Louis, MO). The vials were then placed in light-tight containers and transferred for 1 h to a gently stirred water bath preheated to 24°C to facilitate the loading of Fura-2 into retinal cells. All subsequent procedures were carried out at room temperature (~22°C).

Fluorescence experiments

The intact retina was chosen as a preparation in which the signal from a large number of rods could be summed. This ensured an acceptable ratio of signal-to-noise while keeping the required concentration of dye loaded to a minimum and at the same time allowing the intensity of stimulation to remain in the normal operating range of the rod. We depended on the rationale that the high concentration of rhodopsin in the outer segments would provide a powerful screen against the detection of fluorescence emanating from other parts of the retina (an assumption we put to the test; see Results).

The apparatus used to measure fluorescence from loaded retinas was a modification of that used by Ratto et al. (1988). Briefly, loaded retinas were washed in the dye-free control solution, then mounted receptor-side-up on black filter paper and placed into the recording chamber inside a light-tight faraday cage (Fig. 1). A circular patch, 5.5 mm in diameter encompassing approximately 200,000 rods, was illuminated by light that alternated between 340 and 380 nm every 110 ms. Ultraviolet illumination from a regulated xenon-arc source (ILC Technology, Sunnyvale, CA) served both to stimulate Fura-2 fluorescence and to isomerize approximately 10,000 rhodopsin molecules per second per rod. (The collecting area of a frog rod under end-on stimulation was calculated from data on circular dichroism and absorption of rhodopsin in toad rods (Hárosi, 1975), adjusted for the difference in rod size. For stimulation at 340 or 380 nm, the collecting area of a 70 μm long bullfrog rod is 10 μm^2.) Fluorescence passed through a bandpass filter centered at 500 nm and was counted by a photomultiplier (Thorn EMI, Hayes, UK) in a cooled housing (Pacific Instruments, Concord, CA).

Because the fluorescence we measure arises from so many rods, it is an average that reflects the response of both red and green rods. Eighty-five to ninety percent of the signal comes from red rods, however, because they comprise that percentage of all rods (Rosenkranz, 1977). Moreover, both types of rods have very similar response kinetics (Matthews, 1983) and both should be saturated by the actinic light. (Cones should not contribute significantly because of the small size of their outer segments, the fact that the rod outer segments partially shield them, and because they comprise only about 10–20% of the photoreceptors.) In addition, the response kinetics of rods are very stereotypical (Baylor et al., 1979), particularly during saturating illumination. Hence, we expect the calcium concentrations we measure to be representative of individual rod cells even though they are spatial averages.

Absolute stimulus intensities were determined regularly by placing a calibrated photometer (IL-1700, International Light, Newburyport, MA) in

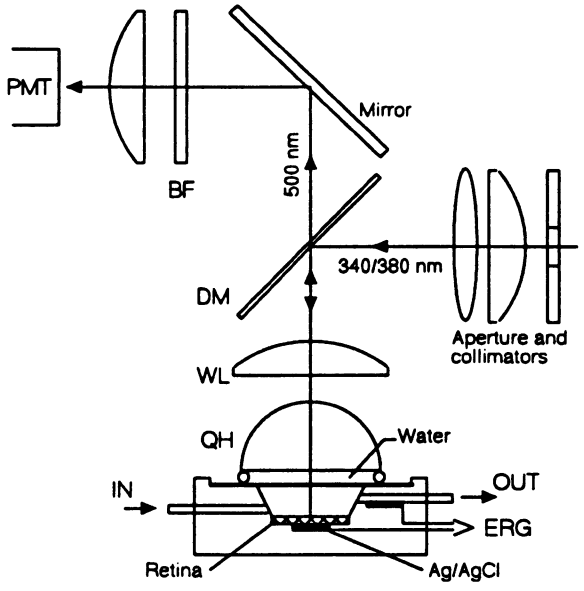

FIGURE 1 Schematic arrangement inside the Faraday cage for illuminating the retina while perfusing it and recording the electroretinogram. Incident UV light is collimated then reflected down onto the retina by a dichroic mirror (DM), passing through a condensing system comprising a weak lens (WL) and a quartz hemisphere (QH). This lens is separated from a thin glass coverslip by a neoprene O-ring; the space between them is filled with distilled water to reduce reflection. In this way, a circular patch of retina 5.5 mm in diameter is evenly illuminated. Ag/AgCl electrodes record the transretinal potential. Arrows in and out of the chamber show the path of the perfusing medium. Fluorescence at around 500 nm is passed by the dichroic mirror and arrives at the photomultiplier (PMT) after passing through a bandpass filter centered around 500 nm (BF) and a weak lens.

the position of the retina in a modified version of the recording chamber. During each experiment, stimulus intensities were continuously monitored with a UV-sensitive diode (S-1226, Hamamatsu, Hamamatsu City, Japan) placed in the path of light reflected from the main stimulation beam.

Up to six different solutions could be delivered to the retina during an experiment. Perfusion was driven by gravity, and changes were complete 1 min after switching. Autofluorescence was measured after quenching Fura-2 fluorescence with manganese (Grynkiewicz et al., 1985). Quenched retinas were indistinguishable from unloaded retinas in their fluorescent properties. Manganese had no effect on unloaded retinas. Photoreceptor responses were monitored with Ag/AgCl electrodes above and below the retina that recorded the electroretinogram (ERG).

A slow, monotonic fall in the fluorescence elicited by both stimulating wavelengths tended to occur at the beginning of our original experiments. The decline was of equal magnitude at both stimulating wavelengths. Because Fura-2 AM fluoresced equally brightly when stimulated by either 340 or 380 nm, we attributed the slow fall to the persistence of unhydrolyzed dye that was slowly leaking out of the retina. We learned to perfuse the retina for at least 20 min before recording data. The decline in signal caused by loss of Fura-2 AM had fallen to a negligible rate by that point and so does not affect the data we present here.

The pentapotassium salt of Fura-2 (Molecular Probes) was calibrated in vitro using the same recording chamber and stimuli described above. Fura-2 was dissolved to 1 μM in 110 mM KCl, 12 mM NaCl. Calcium-free solution contained 5 mM EGTA (ethylene glycol-bis(β-aminoethyl ether) *N,N,N',N'*-tetraacetic acid). The high calcium solution contained 1.5 mM $CaCl_2$. An additional solution was used to test the validity of the calibrations. It typically contained about 170 nM free calcium using a mixture of 1.3 mM calcium and 1.5 mM EGTA. (The dissociation constant of EGTA for calcium at 20°C, pH 7.6 is 26 nM: Martell and Smith, 1974.) All solutions were buffered at pH 7.6 with 3 mM HEPES (*N*-2-[hydroxyethyl]piperazine-*N'*-[-2-ethanesulfonic acid]) and titrated with *N*-methyl *d*-glucamine. Calibrations in which the expected and measured value of free calcium (using the expected in vitro dissociation constant of Fura-2 for calcium of 135 nM) for the validating solution differed markedly were not used.

The calibration parameters are $R_o = 1.02 \pm 0.01$, $R_m = 42.0 \pm 2.7$, and $F = 17.5 \pm 1.5$ ($n = 6$). (All values in this paper are reported mean ± SEM.) We shall use R_o, R_m, and F throughout to represent R_{min}, R_{max}, and S_{f2}/S_{b2}, respectively, of Grynkiewicz et al. (1985). R_o is the ratio of fluorescence elicited by 340-nm illumination to that elicited by 380-nm illumination in the absence of calcium. R_m is the equivalent ratio measured at saturating calcium concentrations. F is the ratio of the fluorescence elicited by 380-nm illumination in the absence of calcium with respect to that measured at saturating calcium concentrations.

Suction electrode experiments

The current circulating between the outer and inner segments of single rods was recorded with the virtual ground/suction electrode method developed by Baylor et al. (1979). Suction electrode experiments were performed in the same room and under the same conditions as fluorescence experiments, usually with cells of the same animal and often at the same time.

Suction electrodes were made from cleaned, nonheparinized hematocrit tubes (02–668–68, Fisher Scientific, Pittsburgh, PA). Double-pulled tubes were scored with a diamond knife and then snapped to produce tips that were clean cut and had outside diameters of 15–20 μm. The tips were melted so that they were smooth and had an inner diameter of approximately 6 μm, and were then coated with γ-methacryloxypropyltrimethoxysilane (Sigma, see Tsien and Rink, 1980) to prevent cell sticking. Electrical connections were made via agar bridges (2–3% wt/wt) connected to calomel electrodes that we constructed (Cobbold, 1974). Photocurrents were low-pass-filtered at 9.8 Hz and sampled at least every 25 ms. Residual noise at 60 Hz was virtually eliminated by driving the bath at 60 Hz but 180° out of phase with the noise.

Stimuli illuminated a 150 μm by 50 μm rectangular area centered on an isolated rod with 565 nm light from a narrow-band LED. Absolute stimulus intensities were determined with the IL-1700 photometer (rod-collecting area at 565 nm for side-on stimulation was 11 μm^2).

Imaging

Fluorescence imaging of retinal slices and isolated rods was performed with the dynamic ratio imaging system described by Tsien and Harootunian (1990). Slices and isolated cells were prepared from loaded retinas. Light intensities required for satisfactory images were many times brighter and longer in duration than those required for calcium measurements in intact retinas. In addition, it was impractical to shield the cells from the dim ambient lighting of the imaging apparatus. Under these conditions, rods are expected to be completely light-adapted.

Solutions

Fresh solutions were made for each day's experiments. The control solution contained 94 mM NaCl, 27 mM $NaHCO_3$, 3.5 mM KCl, 0.6 mM $MgCl_2$, 0.6 mM $MgSO_4$, 1.0 mM CsCl, 1.5 mM $CaCl_2$, 9 mM glucose, 1 mM ascorbic acid, 1 mM Na-pyruvate, 10 mM Na-aspartate, and 3 mM HEPES. The caesium, which blocks the voltage-dependent channels of the inner segment (Fain et al., 1978), was added in all suction pipette experiments to improve resolution of exchange currents (Yau and Nakatani, 1985). It was only used in a minority of fluorescence experiments, where it was found to have no noticeable effect on measured calcium changes. Aspartate isolated the pIII component of the ERG by abolishing light responses in all retinal neurons except photoreceptors (Furakawa and Hanawa, 1955). Pyruvate and ascorbic acid were added to counter possible toxicity from formaldehyde produced as a byproduct of intracellular hydrolysis of Fura-2 (see Korenbrot and Miller (1989), who show that the toxicity of AM esters loaded into rods is not a serious concern).

The Ca^{2+}-free solution was identical to the control solution except for the exclusion of $CaCl_2$ and inclusion of 5 mM EGTA. The Fura-2 signal was usually quenched in a solution identical to the control solution apart from the substitution of 5 mM $MnCl_2$ for $CaCl_2$ and the addition of 0.5 mM IBMX (3-isobutyl-1-methylxanthine), an inhibitor of the cGMP phosphodiesterase in rod outer segments that has been shown to increase outer-segment permeability to manganese (Capovilla et al., 1983). In later experiments, we found that IBMX could be omitted from this solution without significant effect. For the set of experiments where the Fura-2 signal was quenched immediately after exposure to the Ca^{2+}-free solution, the quenching solution was identical to the Ca^{2+}-free solution, but 7.5 mM $MnCl_2$ was added. The higher concentration of added manganese compensated for the fraction of it that would be bound by EGTA. The normal/IBMX solution, used to achieve high internal calcium levels, was the same as the control solution with the addition of 0.5 mM IBMX and, in some instances, 10 μM of the calcium ionophore, ionomycin (Calbiochem, La Jolla, CA). The guanidinium/IBMX solution contained 134 mM CH_5N_3-HCl, 1.5 mM $CaCl_2$, 3.5 mM K-aspartate, 0.5 mM IBMX, 9 mM glucose, and 3 mM HEPES. All solutions had a pH of 7.5–7.6. Solutions were titrated with *N*-methyl *d*-glucamine when necessary.

The membrane-permeable, heavy-metal chelator TPEN (*N,N,N',N'*-tetrakis(2-pyridylmethyl)ethylenediamine), Molecular Probes) (Arslan et al., 1985) was added to the above solutions to a concentration of 50 μM, when noted. In addition, 1 mM EGTA was included in all solutions used in later experiments to mitigate the potential influence of heavy metals that can be bound by Fura-2 (Grynkiewicz et al., 1985). The appropriate free calcium concentration in each solution was maintained by adding calcium sufficient to compensate for the presence of EGTA. Neither TPEN nor EGTA changed our results.

RESULTS

Fura-2 measures $[Ca^{2+}]_i$ erroneously using in vitro parameters

Classical determinations of calcium concentrations with Fura-2 use the ratio method described by Grynkiewicz et al. (1985). The fluorescence ratio is defined as the fluorescence elicited by 340-nm illumination divided by that elicited by

380-nm illumination, after appropriate corrections for autofluorescence have been made. Fig. 2, *A* and *B* show the average time course of fluorescence elicited by each stimulus wavelength from three dark-adapted retinas. They represent the average of a series of stimulations of each retina, each separated by 1 min (ample time for the photocurrent to recover completely, according to suction pipette measurements on loaded rods; McCarthy, 1993). The ratio appears in Fig. 2 *C*. The corresponding photocurrent of seven isolated rods loaded with Fura-2 is shown in Fig. 2 *D*. The stimulus in each case was a 6-s step of illumination that isomerized 10,000 rhodopsin molecules per second per rod. Within 250 ms of the onset of illumination, all cyclic GMP-gated channels in the outer segment are shut and a ratio of 4 is measured. During the next 6 s, cyclic GMP-gated channels remain shut and the exchange current and fluorescence ratio decline. If the same behavior were to continue, one would expect a final, steady-state fluorescence ratio of 2.5, as judged by eye. Experiments in which actinic stimuli were presented for 30 s confirmed this (Fig. 3 *A*) as did experiments in which the stimuli were presented for 60 s (Younger, 1991), steady-state ratios being achieved within 20–30 s (Younger, 1991).

On the basis of the in vitro calibration parameters, a final, steady-state ratio of 2.5 suggests that $[Ca^{2+}]_i$ is approximately 65% of the calcium dissociation constant of Fura-2: on the order of 100 nM. Yet, because the action of the Na^+:Ca^{2+}, K^+ exchange mechanism is expected to reduce the cytoplasmic free calcium concentration to less than a nanomolar (Cervetto et al., 1989), we tested whether the final, steady-state ratio truly reflects an absence of free calcium by exposing retinas to a calcium-free perfusate (containing EGTA and no added calcium).

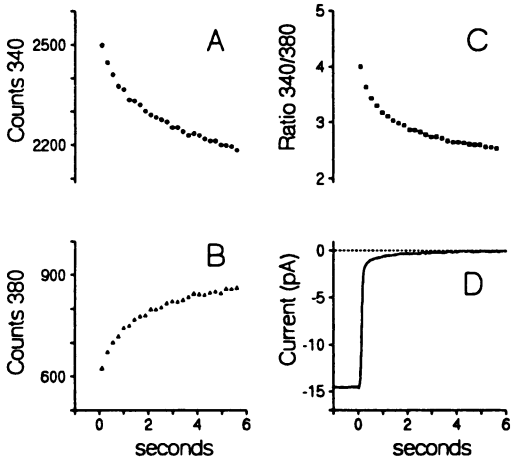

FIGURE 2 The fluorescence evoked from dark-adapted retinas and the photocurrent recorded from isolated Fura-2-loaded rods. The fluorescence elicited (*A*) by 340 nm illumination and (*B*) by 380 nm stimulation after corrections for autofluorescence. Fluorescence is displayed as the number of counts registered by the photomultiplier during a 100-ms period. (*C*) The ratio of the data in *A* to those in *B*. These data are the average of 165 separate trials on three retinas. All were exposed to the control solution, and 50 μM TPEN was added. (*D*) The average circulating current recorded in the control solution from 35 trials on seven isolated rods from 5 different frogs. The slow relaxation of the circulating current to zero is a result of the action of the Na^+:Ca^{2+}, K^+ ion exchange mechanism. The stimulus in all cases isomerized approximately 10,000 rhodopsin molecules/rod/s for 6 s and was repeated every minute.

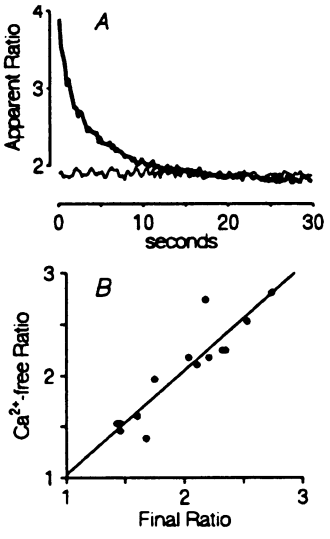

FIGURE 3 The fluorescence ratio falls to a value during saturating illumination that is the same as measured during perfusion with the Ca^{2+}-free solution. (*A*) The average fluorescence ratio measured from four, 30-second trials with a single retina exposed to the control solution (thick trace) and three trials when the retinas had been exposed to the Ca^{2+}-free solution for several min (thin trace). (*B*) The relationship between the final, steady-state ratio for 14 retinas exposed to the control solution and the fluorescence ratio measured from the same retinas while they were exposed to the Ca^{2+}-free solution. The regression line, determined by the least-squares method, has a slope of 1.02 and an intercept of 0.05 (R^2 = 0.84).

Fig. 3 *A* reveals no significant difference between the ratio measured at steady state after several minutes of exposure to the Ca^{2+}-free medium (thin trace) and the asymptote of the ratio in bright light in the control solution (thick trace), implying that the free calcium concentration is the same in both cases. The results of 14 additional experiments of this type are shown in Fig. 3 *B*. In each experiment, the asymptote of the fluorescence ratio in bright light was judged by eye while the retina was exposed to the control solution. It was again determined when the same retina was exposed for several minutes to the Ca^{2+}-free medium. The equality of the ratios of each such pair is made clear by the unity slope of the least-mean-square regression line fitted to the data. If the calcium concentrations measured by Fura-2 were not the same during saturating illumination and while perfused with the Ca^{2+}-free medium, we should not expect such a strong correlation.

After prolonged exposure to the Ca^{2+}-free solution, free calcium in the rod outer-segment cytosol would decline to near zero. Such a bathing medium causes many outer-segment channels to open (Hodgkin et al., 1985), allowing the extracellular and intracellular fluids to approach passive equilibrium. Thus, we should expect that saturating illumination causes the cytosolic free calcium concentration to fall to a value near zero.

It has been suggested, on the contrary, that cytosolic free calcium does not fall below 100 nM because the Na^+:Ca^{2+},

K^+ exchange mechanism inactivates (Schnetkamp et al., 1991; Schnetkamp and Szerencsei, 1993). To test this notion, we performed several experiments in which we added the calcium ionophore ionomycin to the Ca^{2+}-free solution. This technique should bypass any inactivation of the exchange mechanism and bring calcium into passive equilibrium, yet we never observed any further fall in the ratio. This failure of ionomycin to change the ratio is further evidence that cytosolic calcium is close to zero in the Ca^{2+}-free solution, and that the exchange mechanism does not inactivate.

We set out to examine why the signal from Fura-2 in the retina might be yielding values for $[Ca^{2+}]_i$ that are in error. As is common with studies that use Fura-2, we first attempted to calibrate the dye parameters in situ (see Williams and Fay (1990) for a discussion of in situ calibrations). The average value of R_o in situ, determined while retinas were perfused with the Ca^{2+}-free solution, was 2.0 ± 0.1 in 29 experiments.

To determine R_m and F, retinas were perfused with solutions designed to increase cytoplasmic free calcium concentrations: they contained the cyclic GMP phosphodiesterase inhibitor IBMX (Cervetto and McNaughton, 1986). Some also included ionomycin, which did not have any additional effect on the ratios we measured. When retinas were exposed to the normal/IBMX perfusate, the fluorescence ratio increased rapidly and R_m averaged 13.0 ± 1.1 in eight such experiments. The apparent value of F for the same experiments was 2.0 ± 0.1. Six similar experiments with retinas perfused with the guanidinium/IBMX solution yielded an R_m of 11.5 ± 1.2 and an F of 2.1 ± 0.2. The substitution of guanidinium for sodium ensured that the Na^+:Ca^{2+}, K^+ exchange mechanism could not extrude calcium from the outer segment (Nakatani and Yau, 1988). Even exposing retinas to an isotonic calcium/IBMX solution (emulating the technique of Hodgkin et al. (1987), who estimated a rise in total calcium of 1 mM) failed to produce a higher value of R_m.

The in situ parameters are inconsistent with a single, well behaved form of Fura-2

The parameters R_o, R_m, and F are significantly different in situ from those in vitro. We could simply have used these in situ parameters to calculate free cytosolic calcium but, because we wanted to be confident of the kinetics of $[Ca^{2+}]_i$ changes and to be certain that the signal we measured truly represented outer-segment $[Ca^{2+}]_i$ and not calcium in other parts of the retina, we devised a test to determine whether the in situ parameters were accurate.

For a given total amount of Fura-2, fluorescence elicited by each excitation wavelength may be written as

$$U = U_o + U_d b \qquad V = V_o + V_d b, \tag{1}$$

where U and V are the Fura-2 fluorescence elicited by 340- and 380-nm illumination, respectively. U_o and V_o are the Fura-2 fluorescence that would be emitted for each wavelength if all available Fura-2 were in the calcium-free form. U_d and V_d are the difference for the appropriate wavelength between the fluorescence that would be emitted if all the dye were in the calcium-bound form and that which would be emitted if it were all in the calcium-free form. The variable b represents the fraction of available Fura-2 that is in the calcium-bound form. (Writing $b = [Ca^{2+}]_i/(K_d + [Ca^{2+}]_i)$ would lead to the classical expression for calcium (Grynkiewicz et al., 1985).) Simple algebraic manipulation of Eq. 1 results in an expression relating the fluorescence elicited by 340-nm illumination to that evoked by 380-nm illumination.

$$U = mV + (U_o - mV_o), \tag{2}$$

where we have defined a slope, m, as U_d/V_d.

In the usual calibration of Fura-2, four observations (the fluorescence evoked by each excitation wavelength in low and saturating calcium) are used to determine three parameters, R_o, R_m, and F. The slope m is a fourth parameter that can be determined from the classical calibration without additional information (see also Poenie, 1990). Unlike the determination of the values of R_o, R_m, and F, determination of m does not require corrections for background fluorescence or autofluorescence and is thus more accurately determined. An examination of Eq. 2 makes it clear that background fluorescence only affects the intercept of the line relating the Fura-2 fluorescence elicited by each stimulating wavelength.

The slope, m, may be measured independently from R_o, R_m, and F. It may also be predicted from those parameters.

$$m \equiv \frac{U_d}{V_d} = \frac{R_m - R_o F}{1 - F}, \tag{3}$$

where

$$R_o = \frac{U_o}{V_o} \qquad R_m = \frac{U_o + U_d}{V_o + V_d} \qquad F = \frac{V_o}{V_o + V_d}.$$

This new parameter gives us some insight into the properties of Fura-2 in rods. Our in vitro calibration parameters yield an expected slope of -1.5 ± 0.3. In experiments with retinas exposed to the control solution, the slope measured from the light-induced change in fluorescence was normally between -1.3 and -1.7 and averaged -1.5. The average fluorescence elicited by 340 nm illumination from eight experiments on retinas in the control solution is plotted with respect to the average fluorescence elicited by 380-nm excitation in Fig. 4. A line with a slope of -1.5 is drawn through the data to demonstrate how well they are described. This strongly suggests that the light-induced change in fluorescence observed in retinas exposed to the control solution originates from a pool of Fura-2 that behaves very much like the in vitro form. On the other hand, the slope predicted from our in situ calibration is approximately -8, using typical values $R_o = 2$, $R_m = 12$, and $F = 2$. That value for the expected slope would not change even if our estimate of the in situ values of R_m and F were in error because the calcium concentration in rods exposed to either the IBMX or isotonic calcium solution had not been high enough to saturate Fura-2.

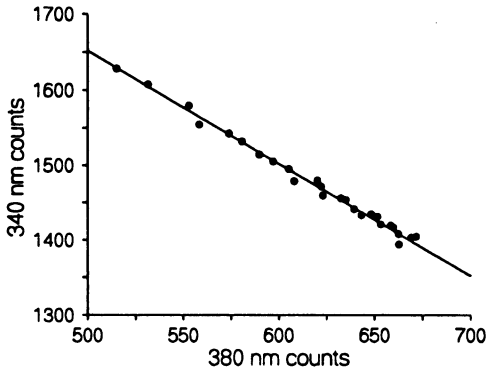

FIGURE 4 The relationship between the fluorescence elicited by 340 nm illumination to that evoked by 380 nm illumination for retinas in the control solution. The data shown are equivalent to those shown in Fig. 2, *A* and *B* but are the average of 8 experiments of 10 trials each. The line through the data was fitted by eye and has a slope of −1.5.

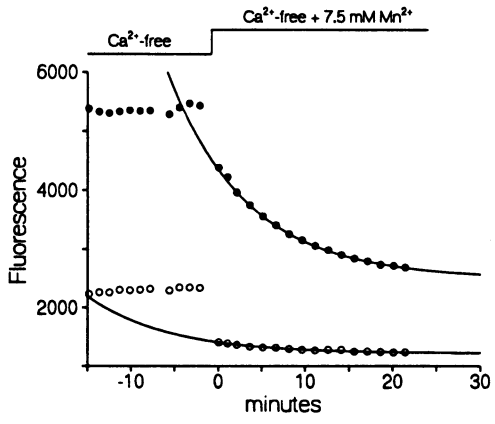

FIGURE 5 During quenching of Fura-2 fluorescence with manganese, two phases of decline in the signal are apparent. A retina in the Ca^{2+}-free solution is exposed to manganese at $t = 0$. The fluorescence evoked by both 340 nm (●) and 380 nm (○) shows an initial fast drop followed by a slower fall. The smooth curve through the 340 nm data is $1050e^{-t/9.2} + 2500$, which through the 380 nm data is $190e^{-t/9.2} + 1215$. The time constant for these functions was determined by the best fit to the result of subtracting the 380 nm data from the 340 nm data. Because the size of the fast fall was about the same at both wavelengths, subtracting the two sets of data left only the contribution from the slower fall.

The fact that the slope predicted from the in situ parameters is not at all consistent with the light-induced behavior of the fluorescence we measure precludes our using the in situ parameters to determine $[Ca^{2+}]_i$.

Distinct pools of Fura-2 are revealed when fluorescence is quenched

Several factors could account for the invalidity of the in situ parameters. The fluorescence we measure could arise from more than one pool of Fura-2, or Fura-2 might bind calcium differently in rods than it does in vitro, or its fluorescent character may be altered by intracellular factors such as viscosity and hydrophobic environments (Roe et al., 1990; Poenie, 1990; Uto et al., 1991). The data and analysis below show that the first of these factors is true.

When Fura-2 is quenched at the end of an experiment, two phases in the fall in signal are apparent. A fraction of the dye signal is quenched rapidly, and the rest of the signal is extinguished much more slowly. In Fura-2-loaded retinas that are exposed to the quenching solution (containing 7.5 mM $MnCl_2$ and 5 mM EGTA) immediately after exposure to the Ca^{2+}-free solution, the two phases are very distinct. Fig. 5 shows a representative record of a quench in such an experiment. There is a significant decrease in fluorescence within the first minute or two, the signal evoked by each wavelength falling by approximately the same amount. The fluorescence elicited by 380-nm illumination is nearly eliminated in this period, whereas the fluorescence elicited by 340 nm is still substantial. Over the subsequent 20 min, the 340-nm fluorescence gradually decreases. We estimated the relative amplitudes of the two phases at the start of the quench for both stimulating wavelengths by fitting the slower phase to a simple exponential function (using the same time constant for both wavelengths). In 15 such experiments, the ratio of the magnitude of the 340 nm fast phase to the 380 nm fast phase was 1.05 ± 0.03. Because the quench is preceded by a prolonged exposure to the Ca^{2+}-free solution, we expect cytosolic free calcium to be close to zero at the beginning of the quench. A pool of Fura-2 that behaves like the in vitro dye should have a fluorescence ratio of 1.02 ± 0.01 at that time. The similarity between the observed ratio and the ratio expected for in vitro dye leads us to propose that the rapidly quenched signal is caused by Fura-2 that is free in the cytosol.

The other pool is quenched much more slowly and accounts for a much greater fraction of the total quenchable fluorescence at 340 nm than it does at 380 nm. The average ratio of fluorescence for this pool in these conditions, while cytosolic calcium is close to zero, is 6 ± 1 (n = 15). Such a result would be consistent with a pool of Fura-2 that is relatively inaccessible to manganese and sensing a calcium concentration several times its dissociation constant for calcium.

We utilized the different rates at which Fura-2's fluorescence is quenched to obtain more direct proof that there is more than one pool and that one of them behaves much like the in vitro form of Fura-2. In Fig. 6, we show that when a Fura-2-loaded retina is exposed to the quenching solution for only 30 s, only the rapidly quenched pool is eliminated. The data plotted in the upper panels (*A* and *B*) are the fluorescence counts evoked by 340 nm at the end of 30 s of stimulation. The lower panels (*C* and *D*) show the counts evoked by the 380 nm stimulus partner. At the time marked by the arrow, the perfusate was switched from the control solution to the quenching solution and then back to the control solution after 30 s. For both wavelengths, the fluorescence is immediately reduced after the switch, but then remains constant. Later in the experiment, the remaining fluorescence is eliminated by continuous exposure to the quenching solution.

The results here confirm those inferred from the data shown in Fig. 5. Some of the Fura-2 in the loaded retina is

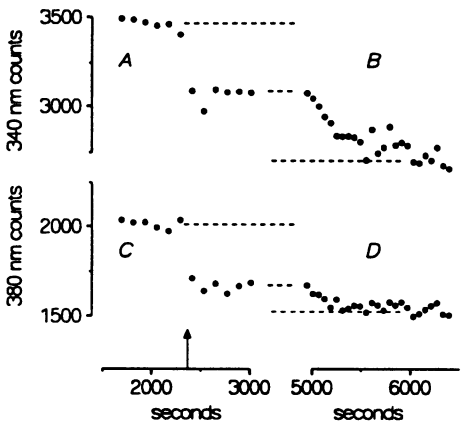

FIGURE 6 Rapidly- and slowly quenched pools can be isolated by briefly exposing the retina to the quenching solution. The data are the fluorescence measured at the end of a 30-s step of saturating light. In *A* (340 nm light) and *C* (380 nm light), the retina was perfused with the control solution except for a 30-s interruption while the quenching solution was presented (indicated by the *upward arrow*). That the fluorescence evoked by both stimulating wavelengths rapidly fell by nearly the same amount (R = 1.1) immediately after the exposure to the quenching solution demonstrates that some Fura-2 is rapidly accessed by manganese. The quenching solution was again presented to the retina at the beginning of *B* and *D*. There was no rapid quench this time, only the gradual extinction of the slowly quenched source of fluorescence.

quenched rapidly. The 340 nm to 380 nm ratio of that pool is 1.1 at the tail end of the 30-s stimuli in this particular experiment. The remaining fluorescence is quenched slowly.

Additional evidence for at least two distinct pools of Fura-2 is shown in Fig. 7. The data here are the typical changes in fluorescence elicited by the 340- and 380-nm components of stimulation both before any Fura-2 is quenched (*open circles*) and after a 30–40 s exposure to the quenching solution (*filled circles*). Before the partial quench, the usual light-induced fall in calcium is clearly indicated by the time-dependent change in fluorescence. But after the partial quench, there is no time-dependent change even though the ERG continued to record normal light responses. This means that the rapidly quenched pool is identical to the pool that senses the light-induced change in calcium. The other pool is calcium-insensitive in the control solution but contributes a constant, ultimately quenchable fluorescence that is the reason our in situ value of R_0 is near 2 rather than 1 as we would expect from our in vitro calibration.

The rapidly quenched pool does have an in situ R_0 value near 1, like the in vitro value. This fact is illustrated in Fig. 8. Panels *A* and *C* are the fluorescence ratios obtained using the final quench level, which includes both the rapidly and slowly quenched sources of fluorescence. The ratios in panel *A* were obtained when the retina was exposed to the control solution, whereas those in *C* were obtained when the same retina was perfused with the Ca^{2+}-free solution. Compare these ratios with those obtained when only the rapidly quenched source of fluorescence is considered (Fig. 8, *B* and *D*). The ratios translate down by 0.9 in each case. In the control solution, the final steady-state ratio is 1.9 when determined from the total quench level, but 1.0 when only the rapidly quenched pool is considered. The ratio in the Ca^{2+}-free solution is 2.1 in the first case and 1.2 in the second.

Earlier, we argued that cytosolic calcium falls to near zero during saturating illumination because the fluorescence ratios measured when retinas are perfused with the Ca^{2+}-free solution are the same as the steady-state ratios measured

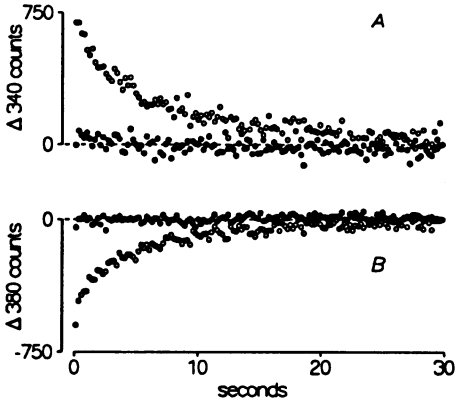

FIGURE 7 The light-induced change in fluorescence is eliminated by a 30-s exposure of the retina to the quenching solution. The data shown are from a partial-quench experiment of the type shown in Fig. 6. The average light-induced change in fluorescence evoked from five trials with a retina exposed to the control solution before the presentation of the quenching solution is shown as open circles (*A*, 340 nm excitation; *B*, 380 nm excitation). When the control solution is restored after a 30-s exposure to the quenching solution, the ERG continues to record normal light responses (not shown), but the light-induced change in fluorescence is abolished (the average of four trials is shown). In this experiment, the fluorescence ratio measured from the rapidly quenched pool at the end of a 30-s step of saturating light was 1.3.

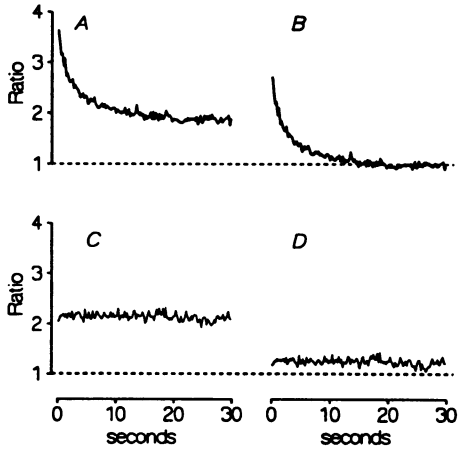

FIGURE 8 Ratios determined from the rapidly quenched pool alone are lower than the ratios determined after all fluorescence is quenched. With respect to the autofluorescence of the retina, measured after all other sources have been quenched, the average fluorescence ratio from three trials with a retina exposed to the control solution fell to 1.9 at the end of a 30-s step of saturating illumination (*A*). Its value was 2.1 when the retina was perfused with the Ca^{2+}-free solution (*B*). The same data give a final fluorescence ratio of 1.0 for the control solution (*C*) and 1.2 for the Ca^{2+}-free solution (*D*) when determined relative to the fluorescence remaining after elimination of the rapidly quenched pool by a 30-s presentation of the quenching solution.

during saturating illumination of retinas perfused with the control solution. Now, having seen that the ratios we obtain for the rapidly quenched pool are indistinguishable from the in vitro R_0 value of 1.0 both at the end of 30 s of saturating illumination and during exposure to the Ca^{2+}-free solution, it seems clear that calcium really does fall to zero. Moreover, the fact that the rapidly quenched pool of Fura-2 is the only light-sensitive pool when retinas are exposed to the control solution, and that its 340 nm/380 nm slope is the same as would be predicted from our in vitro calibrations, it is apparent that the the rapidly quenched pool is identical to the in vitro form of Fura-2, although final proof of this requires values for R_m and F, which we determine below.

Fluorescence from sources outside the outer segment does not cause the error

The slowly quenched pool of Fura-2 is consistent with a compartmentalized store either within rod outer segments or elsewhere in the retina. Compartmentalization of Fura-2 within a cell is not uncommon (Roe et al., 1990), nor is the possibility that we might measure fluorescence from parts of the retina other than the outer-segment cytosol very surprising. Thus, we performed experiments to determine if significant fluorescent signal might emanate from other cells in the retina or from regions of the rod other than the outer-segment cytosol (the outer-segment disks or the inner segment, for example).

We used a fluorescence imaging system that allowed us to measure the relative fluorescent intensities elicited by 340- and 380-nm light from slices of retinas and from isolated rods to make an estimate of the relative dye loading in each region of the retina. (Slices were obtained by making two parallel cuts through Fura-2-loaded retinas. Each cut exposed a retinal cross section by cleaving the retina from the photoreceptor layer through to the ganglion cell layer.) By far the brightest region of every slice was its photoreceptor layer. Fluorescence from the remainder of the retina was unmeasurable above background noise, except for an occasional ganglion cell. The higher concentration of Fura-2 in rod cells is consistent with the measurements of Ratto et al. (1988), who found 67% of loaded Fura-2 to be in the rod outer segments. As they pointed out, this is expected given that only photoreceptors and ganglion cells are in direct contact with the loading solution and that the total surface area of the rods is much greater than that of any other cell type in the retina. Within isolated rod cells and in the photoreceptor layer of slices, the inner segment region was approximately 3 times brighter than the outer segment region for both 340- and 380-nm excitation.

The difference in intensity might suggest that Fura-2 is several times more concentrated in the inner segment than in the outer segment. But the cytosol accounts for only about half the total volume of an outer segment. The remainder of the outer segment is occupied by lipid bilayer disks. Moreover, absorption by rhodopsin in the outer segment attenuates the Fura-2 signal there. With these factors in mind, one finds that if the cytosolic concentration of Fura-2 were the same in the inner and outer segments, the inner segment should appear 2.5–3 times as bright as the outer segment when viewed side-on, as we observe. We conclude, therefore, that the cytosolic concentrations of Fura-2 in the inner and outer segments must be nearly the same, in agreement with the cell-fractionation measurements of Ratto et al. (1988).

Given the distribution of Fura-2 in the retina, we can calculate the amount of screening rhodopsin provides in our experiments on the intact retina. Rhodopsin screens both the incoming UV light and fluorescence emitted at 500 nm. For a rod whose outer segment is 70 μm long, we calculate that 97% of the fluorescence collected stems from the outer segment. However, we did not rely on this calculation. We tested it and resolved with certainty that light-induced changes in fluorescence originate purely in the outer segments.

In the usual experiments, we mounted retinas on circular pieces of filter paper so that the photoreceptors were nearest the stimulus (photoreceptor-side-up). We altered this configuration in several experiments in a manner similar to that of Ratto et al. (1988). A retina was sandwiched between two filter-paper annuli. Experiments began with the retina mounted photoreceptor-side-up. Midway through the experiment, the retina was inverted so that the proximal layers of the retina were now closer to the stimulus (photoreceptor-side-down). After taking readings, Fura-2 was quenched and residual fluorescence was measured in both orientations. In both the photoreceptor-up and photoreceptor-down configurations, the fluorescence contribution from the outer segments should be nearly equivalent because the remainder of the retina is fairly transparent to the excitation and emission wavelengths (Fig. 9 *A*). However, any contribution from the inner segments and from other retinal neurons should be much greater in the photoreceptor-down configuration. In both configurations, the contribution from the outer segments should be the same.

The total fluorescence elicited from the retina was approximately 3 times brighter in the photoreceptor-down orientation than in the photoreceptor-up configuration, slightly greater than that found by Ratto et al. (1988). The greater total fluorescence in the photoreceptor-down configuration suggests that shielding of Fura-2 fluorescence elicited from the inner segment and the rest of the retina by the rhodopsin in the outer segment is significant and is consistent with our calculations. The light-induced change in fluorescence when the retina was mounted photoreceptor-side-down was approximately 70% of that from the photoreceptor-up configuration. The average light-induced change in fluorescence in each configuration appears, normalized, in Fig. 9 *B*. The time courses are strikingly similar. The decrease in intensity may be caused by loss of rod cells incurred when inverting retinas, or from ultraviolet absorption by the retina. If a significant part of the light-induced change in fluorescence had originated from someplace other than the outer segments, we would have seen a greater light-induced change in the photoreceptor-down configuration and should have expected the kinetics to be weighted toward the change in calcium

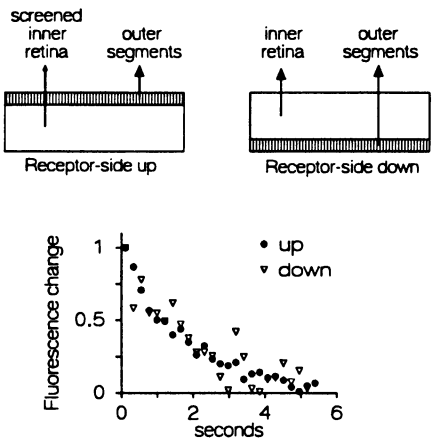

FIGURE 9 The light-induced change in fluorescence from a Fura-2-loaded retina in both photoreceptor-up (●) and photoreceptor-down orientations (△). The configurations are diagrammed in the upper part of the figure, the size of the arrow heads indicating that fluorescence from the inner retina would be screened by outer segments in the photoreceptor-up configuration. Each data point in the lower panel was calculated by measuring the difference between the fluorescence in a particular 100 ms counting period and the last counting period of the 6-s stimulation. Data from both stimulating wavelengths are averaged to form each point. Each trace is the average of 30 trials. The change in fluorescence in the photoreceptor-down configuration was 30% smaller, so the two traces have been normalized for comparison of kinetics.

sensed by the Fura-2 outside the rod outer segments. The observation that the photoreceptor-down fluorescence followed the same time course but was less intense than the photoreceptor-up fluorescence demonstrates that the light-induced change in fluorescence for each configuration originates solely in the outer segments of rods.

We can also be sure that in our usual photoreceptor-up configuration better than 90% of the total fluorescence arises from the rod outer segment layer. This latter result suggests that the slowly quenched pool of Fura-2 is associated with the rod outer segments. It may be contained within the disks of the outer segment and sense a high calcium concentration there (Szuts and Cone, 1977; Schröder and Fain, 1984; Somlyo and Walz, 1985). Yet the possibility that it is a distinct cytoplasmic pool or is contained in damaged cells of the rod mosaic cannot be discounted.

Anomalous properties of the other source of fluorescence

Wherever the slowly quenched pool resides, some of its properties can be determined. Fig. 7 demonstrates that there is no light-induced change in fluorescence arising from the slowly quenched pool of Fura-2 when the retina is exposed to the control solution. That is not the case when a Fura-2-loaded retina is exposed to the IBMX solution that elevates the cytosolic free calcium concentration in rod outer segments by inhibiting phosphodiesterase activity.

The average total fluorescence measured from eight retinas exposed to the normal/IBMX perfusate is shown in Fig. 10, *A* and *B*. Like our previous data, the fall in fluorescence elicited by 340-nm stimulation is accompanied by an increase in the fluorescence elicited by 380-nm stimulation, indicating a fall in cytosolic free calcium. But unlike data obtained from retinas exposed to the control solution, these data cannot be described by Eq. 2. The change in the 340 nm elicited fluorescence is not a scaled, mirror image of the change in the 380 nm elicited fluorescence, as demonstrated in Fig. 10 *C*. The fact that the data deviate from a straight line means that they do not arise from a single, well behaved pool of Fura-2. (IBMX had no effect on unloaded retinas.)

Having already established the existence of more than one pool of Fura-2 in the rod outer segment layer, we looked to see if the anomalous fluorescence apparent in the presence of IBMX could be assigned to either the rapidly quenched or slowly quenched pool. After extinguishing the rapidly quenched pool by a 30-s exposure to the quenching solution, the fluorescence measured in the control solution was consistent with the data shown in Fig. 7; no change was observed for either wavelength. We then exposed the retina to IBMX and recorded the fluorescence shown in Fig. 11 *A*. Note that although the fluorescence elicited by 380-nm light hardly changed at all, the fluorescence elicited by 340-nm light changed significantly during stimulation, demonstrating that the slowly quenched pool, although unresponsive in the presence of the control solution, is responsive in the presence of IBMX.

More important, the anomalous fluorescence can be entirely attributed to the slowly quenched pool. After a partial quench, 380-nm light evoked no measurable change in fluorescence from the slowly quenched pool. It follows, there-

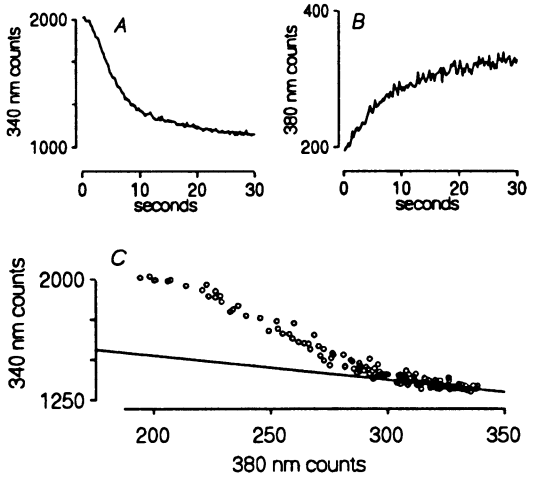

FIGURE 10 The average fluorescence evoked by 30 s of stimulation from eight retinas in the normal/IBMX solution. There was little variation in the kinetics of the light-induced change in fluorescence between each retina. The time course of the measured fluorescence evoked (*A*) by 340 nm light and by (*B*) 380 nm light. (*C*) The relationship between the 340 and 380 nm data. The line drawn through the lower part of the data has a slope of −1.5. Data recorded from the same retinas when exposed to the control solution would lie on the line and overlie the lower portion of the data shown here. Clearly, this is not true of the data recorded in the presence of IBMX.

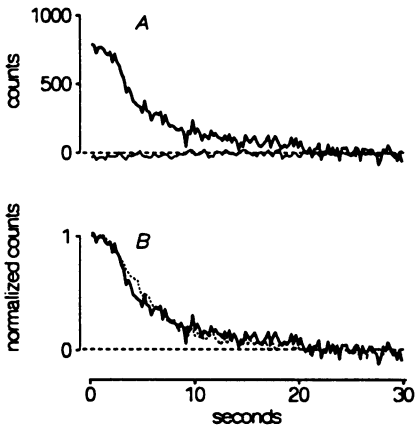

FIGURE 11 The anomalous component of the signal recorded from retinas exposed to IBMX arises from the slowly quenched source of fluorescence. (*A*) The change in fluorescence evoked by 340-nm light (*thick* trace) and 380-nm light (*thin* trace) after a 30-s exposure to the quenching solution. Unlike the data shown in Fig. 10, there is very little change in the 380 nm evoked fluorescence. When the 380-nm signal shown in Fig. 10 *B* is multiplied by −1.5 (the 340–380 nm slope of the rapidly quenched pool) and subtracted from the 340 nm signal shown in Fig. 10 *A*, the dashed trace shown here in panel *B* is obtained. When normalized to account for a 20% difference in absolute amplitude, the dashed trace superimposes well on the normalized reproduction of the 340-nm signal shown in *A*. This indicates that the anomalous fluorescence arises from the slowly quenched pool.

fore, that the change in fluorescence evoked by 380-nm light before the partial quench must come from the rapidly quenched pool. If we assume that the rapidly quenched pool is as well behaved in the presence of IBMX as it is in the control solution, we can determine its contribution to the total fluorescence elicited by 340-nm light. To do this, we simply multiply the change in 380 nm-evoked fluorescence by −1.5, the value of m for the rapidly quenched pool (see Eq. 2). If our assumption is correct, the anomalous component will be the difference of the total fluorescence and our estimate of the contribution from the rapidly quenched pool. Moreover, the anomalous fluorescence estimated in this way should be identical to the fluorescence measured directly from the slowly quenched pool in the presence of IBMX. The traces shown in Fig. 11 *B* demonstrate that this is the case. The thick trace is the normalized change in fluorescence evoked from the slowly quenched pool by 340-nm light (it is derived from the data shown in Fig. 11 *A*). The dashed trace is our estimate of the anomalous component of the fluorescence data shown in Fig. 10, *A* and *B*. Both traces are normalized because they are averages from different experiments, but clearly the kinetics are identical. In individual experiments where retinas were exposed to IBMX both before and after a partial quench, the difference in fluorescence, although noisy, had properties identical to those of the rapidly quenched pool in the control solution; the fluorescence evoked by 340-nm light was −1.5 times the fluorescence evoked by 380-nm light. It is clear from these results that the anomalous fluorescence arises solely from the slowly quenched pool and that the rapidly quenched pool is well behaved even in the presence of IBMX.

Cytosolic free calcium during saturating illumination of rod outer segments

The fact that the rapidly quenched pool is always well behaved allows us to determine its values for R_m and F. We did this in several experiments where retinas were exposed to IBMX by subtracting the fluorescence evoked after a partial quench from that evoked before the partial quench. Our estimates of the value of R_m, derived from the fluorescence measured at the onset of stimulation, ranged from 25 to 50. Values for F ranged from a minimum of 6.5 to an indeterminate number greater than 10. These parameters are closer to those we obtained in our in vitro calibrations ($R_m = 42.0 \pm 1.5$, $F = 17.5 \pm 1.5$) than in our original in situ calibration ($R_m \approx 12$, $F \approx 2$), which did not acknowledge multiple pools of Fura-2. When coupled with the fact that the change in fluorescence elicited from the rapidly quenched pool by 340-nm light is −1.5 times the change in fluorescence elicited by 380-nm light, as would be predicted on the basis of the in vitro parameters, and the fact that the value of R_o for the rapidly quenched pool is indistinguishable from the in vitro value of R_o of 1, we must conclude that the rapidly quenched pool is composed of Fura-2 that is the same as the classic, in vitro form of Fura-2.

Our results have demonstrated that the light-induced change in fluorescence observed in retinas exposed to the control solution is evoked entirely from the rapidly quenched pool and arises solely from rod outer segments. Hence, the light-induced fall in calcium in the rod outer segments can be determined from the behavior of the rapidly quenched pool by use of the usual ratio method.

$$\frac{[Ca^{2+}]}{K_d} = \frac{R - R_o}{R_m - R} F \qquad (4)$$

K_d is Fura-2's calcium dissociation constant.

The light-induced fall in calcium measured in two representative experiments is shown in Fig. 12 *A*. In both cases, the stimuli were 30-s steps of saturating illumination and the calcium concentrations were derived from the in vitro parameters. These data bracket the range of concentrations we measured under normal conditions and, thus, quantify the precision with which we can report calcium concentrations relative to the dissociation constant of Fura-2 for calcium. The final, steady-state calcium concentration during saturating illumination ranged from −0.03 to 0.09 of the K_d. Calcium concentrations measured from retinas perfused with the Ca^{2+}-free solution showed the same variability and covered the same range. This experiment-to-experiment variability is the dominant source of uncertainty in our method. Hence, based on a likely K_d of 350 nM (see below), the calcium concentration, during either saturating illumination or perfusion with the Ca^{2+}-free medium, is no greater than about 30 nM. In the dark, measured calcium concentrations range between 0.7 and 1.1 of Fura-2's dissociation constant.

Our other source of uncertainty is the variability within an experiment and is shown in Fig. 12 *B* expressed as the SEM

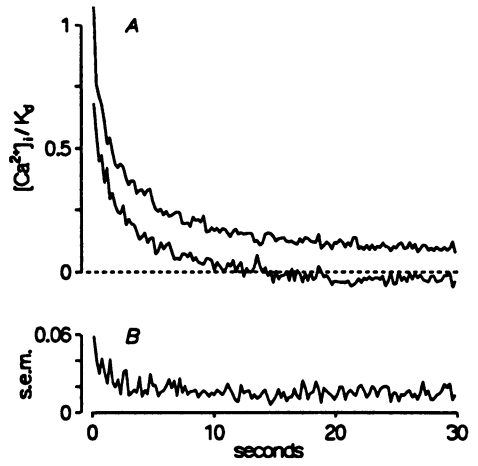

FIGURE 12 The change in cytosolic free calcium concentration produced by a 30-s step of saturating light. (*A*) The light-induced fall in calcium concentration from two experiments is shown to demonstrate the range of values we obtained. The upper trace is the average of six trials, and the lower trace is the average of three trials. Both were calculated from Eq. 4 with the in vitro parameters. (*B*) The SEM of $[Ca^{2+}]/K_d$, which indicates the uncertainty that arises from random noise. Its magnitude varied little from one experiment to the next.

of the calcium concentration relative to the K_d. This uncertainty, which is a small part of our overall uncertainty, is a measure of random noise and is the same in each experiment. In the dark, the value of the SEM ($[Ca^{2+}]/K_d$) is about 0.06, but within 5 s it falls to a steady value between 0.01 and 0.02.

We do not show absolute calcium concentrations in Fig. 12 *A* because we did not measure the dissociation constant of Fura-2 for calcium in rod outer segments directly. Yet, other labs have measured Fura-2's K_d in situations that should be similar to the rod outer segment cytosol. Negulescu and Machen (1990) measured it in parietal cells and reported an in situ value of 350 nM. Groden et al. (1991) measured an in vitro K_d of 236 nM in a solution with an ionic strength of 150 mM, and Uto et al. (1991) evaluated a K_d of 266 nM when the ionic strength was 170 mM. Hence, although we must be cautious of the latter in vitro measures because Konishi et al. (1988) reported that Fura-2's dissociation constant could be three- to fourfold higher in the presence of proteins, we can expect the dissociation constant of Fura-2 in rod outer segments to be between 250 and 350 nM. This suggests that the cytosolic free calcium concentration in darkness is between 175 and 400 nM.

This range of concentrations is also supported by an independent assay of the calcium concentration based on the exchange current we measure. Because the exchange current is first-order, the steady-state cytosolic free calcium concentration near the outer segment's plasma membrane in the dark can be described by the relationship given by Lagnado et al. (1988):

$$[Ca^{2+}] = K_{ex}\frac{J_{ex}}{J_{sat} - J_{ex}}. \quad (5)$$

Here, J_{ex} is the current generated by the exchanger, J_{sat} is its magnitude when saturated, and K_{ex} is its calcium dissociation constant. In the dark, J_{ex} is approximately 2 pA (Fig 13), whereas the saturated exchange current during a brief exposure to the normal/IBMX perfusate is 10 pA (McCarthy, 1993). (It should be noted that the exchanger is voltage-dependent, becoming less efficient when a rod is depolarized, as in the presence of IBMX. We estimate that the appropriate value of J_{sat} at the dark potential is 13–14 pA.) The affinity of the exchanger, K_{ex}, is reported to be 1.6 μM in salamander (Lagnado et al., 1992) and 0.9 μM in bovine rods (Schnetkamp, 1991). Given these parameters, we should expect cytosolic free calcium in the dark to be between 150 and 300 nM, similar to the above estimate.

Independent of the absolute calcium concentrations, we can be confident of the kinetics of the fall in calcium for two reasons. First, Fura-2 has no noticeable effect on the kinetics of the exchange current as shown if Fig. 13. This means that the rod's native calcium-buffering is very large compared with the additional buffering provided by Fura-2. It also means that the calcium kinetics we observe in the intact, Fura-2-loaded retina will differ very little from those of unloaded rods. The other reason to believe that the kinetics we observe are accurate is that the fluorescence ratios we measure ($R \leq 4$) are small with respect to R_m whether it is measured in vitro or in situ from the rapidly quenched pool. Hence, the time course of the change in calcium is essentially the same as the time course of the fluorescence ratio, which is arguably the least variable aspect of our data. That the experiment-to-experiment variability we discussed above does not affect the measured calcium kinetics can be seen in Fig 12 *A* where the upper trace, when shifted downward by 0.12, would have a time course that is indistinguishable from that of the lower trace.

Clearly, calcium in rod outer segments falls slowly, and with a time course similar to that of the exchange current, as we should expect. Moreover, the fact that calcium and the exchange current have kinetics that are simply related allows us to consider how calcium's light-induced dynamics are regulated, a subject we shall discuss in a later paper.

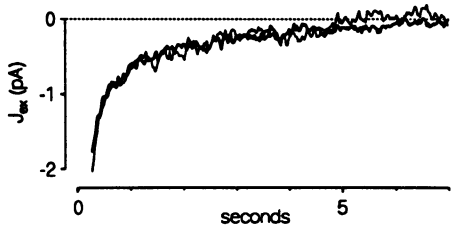

FIGURE 13 The exchange current recorded from Fura-2-loaded rods (*thick* trace) and unloaded rods (*thin* trace). The trace from the loaded cells is a reproduction of that in Fig. 2 *D*. The exchange current from unloaded rods in the control solution, with a 6-s stimulus of 10,000 isomerized rhodopsin molecules per second, is the average of eight cells from five frogs. (Beyond about 6 s, the relaxation of the exchange current is obscured by noise.) The average total light-suppressible current was the same in both cases.

DISCUSSION

The original rationale for using Fura-2 was that it could be loaded into intact retinas and calcium concentrations thereby measured under physiological conditions. Although Fura-2 proved to be less cooperative than was at first hoped, in the end it proved itself to be a capable calcium indicator. The reproducibility of our data indicates to us that the light-induced changes in cytosolic free calcium we report are as representative as possible of those in rods of a living frog.

Our most important finding in terms of light adaptation in vertebrate photoreceptors is the confirmation that $[Ca^{2+}]_i$ falls to near zero during saturating illumination. This initially stemmed from our observation that the fluorescence ratios we measured from retinas exposed to a calcium-free perfusate were the same as those measured after 20–30 s of bright light. It was confirmed by our finding that Fura-2 exists in at least two forms in rod outer segments. One of these is indistinguishable from the classic, in vitro form of Fura-2 and, under normal physiological conditions, is solely responsible for reporting light-induced changes in cytosolic free calcium. When the contribution of that pool is isolated, the usual ratio method shows that calcium is less than 30 nM (using a K_d for Fura-2 of 350 nM).

The time course of the fall in calcium we measure during saturating illumination is slower than, but otherwise consistent with, the light-induced calcium extrusion measured by Miller and Korenbrot (1987). It is also similar to previous reports from our lab (Ratto et al., 1987; Younger, 1991; Younger et al., 1992) and to a recent measure in detached rod outer segments using dextran-Indo by Gray-Keller and Detwiler (1994). The slowness of the light-induced change in calcium has clear implications with regard to how rapidly calcium-dependent light adaptation can develop.

Yet it is our examination of Fura-2 that may be of more interest to people using fluorescent indicators. We show that the second source of fluorescence in Fura-2-loaded retinas emits more brightly in 340-nm light than in 380-nm light. It is responsible for the unrealistically high ratios that led Ratto et al. (1988) to report that cytosolic free calcium does not fall below 140 nM during saturating illumination. Although we cannot state that the fluorescence from the slowly quenched pool arises from only one form of Fura-2, or where the slowly quenched pool resides, the outer segment disks are an obvious candidate. Calcium is thought to be high in the disks (Szuts and Cone, 1977; Schröder and Fain, 1984; Somlyo and Walz, 1985), and Ratto et al. (1988) found that up to 13% of the total dye in Fura-2-loaded rod outer segments could be contained in the disks. Heavy metals such as zinc, which binds to Fura-2 and mimics calcium in some ways, cannot be the source of the second pool because neither TPEN, a membrane-permeable, heavy-metal chelator, nor EGTA in the perfusate eliminated the second pool. Based on our imaging experiments and the shielding provided by rhodopsin, we can also rule out fluorescence from parts of the retina other than the photoreceptors as a major contributor to the second pool. Fura-2 trapped in the extracellular matrix is unlikely to be a factor because we perfused retinas for at least 20 min before recording data. On the other hand, Fura-2 trapped in damaged rods might be a contributor to the second pool. Cones should not contribute significantly, both because their outer segments are small and because they are screened to some extent by rod outer segments. Another possibility comes from the fact that Fura-2 and its BAPTA-derived relatives bind significantly to intracellular proteins and exist in different forms within cells (Chiancone et al., 1986; Konishi et al., 1988; Blatter and Wier, 1990; Bancel et al., 1992; Hove-Madsen and Bers, 1992). Thus, Fura-2 in one of those forms could account for the slowly quenched pool if it were not easily accessed by manganese. Nevertheless, none of these possibilities would alter the fact that the light-induced, physiological change in calcium we report in retinas exposed to the control solution arises only from the classic pool, with all additional sources of fluorescence appearing simply as an insensitive background.

The anomalous fluorescence that is elicited from the second pool in the presence of IBMX is not so easily dismissed. The fact that the fluorescence evoked by 380-nm light does not change whereas the fluorescence evoked by 340-nm light changes significantly is not consistent with a ratio dye like Fura-2 unless the source of this anomalous fluorescence has its isosbestic point near 380 nm rather than near 360 nm as is the case for the in vitro form of Fura-2. Significantly, Bancel et al. (1992) have reported that the excitation spectrum of protein-bound Fura-2 is red-shifted by about this amount with respect to the spectrum of the calcium-free form of Fura-2, although Konishi et al. (1988) report a smaller red shift of only 5–6 nm. Evidence that protein interactions may be a factor in rod outer segments is supported by Gray-Keller and Detwiler (1994), who found that the free salt of Indo-1 dialyzed into detached rod outer segments reports apparent calcium dynamics that are significantly different from those signaled by its dextran-conjugated counterpart, which should be affected less by protein interactions. Hence, although we do not know what causes the anomalous fluorescence, it is possible that noncalcium interactions are responsible. What must be emphasized, however, is that the time-varying fluorescence that we have called the anomalous fluorescence is not present when retinas are exposed to the control solution and, thus, is not a factor in those situations.

Although the initial aim of this study was not to expose the nature of Fura-2 in situ, we have along the way derived a simple means for checking the validity of calcium measurements that may be useful to others using Fura-2 or other fluorescent ratio dyes. The customary approach is to perform a calibration to determine R_o, R_m, and F in situ and substitute these parameters into the traditional ratio equation (Grynkiewicz et al., 1985). If these parameters are substituted into Eq. 3, an expected slope m for the relation between fluorescence at the two stimulating wavelengths is obtained. If the experimental data do not fit this slope, then the in situ calibration is in error and one's experimental protocol must be examined more closely.

We thank Dr. G. M. Ratto for constructing the original version of the fluorescence apparatus and data acquisition software. Drs. R. S. Zucker and Y.-Y. Peng were of great help during the fluorescent imaging procedures. Funding for this study was provided by National Institutes of Health research grant EY03785 to W. G. Owen.

REFERENCES

Arslan, P., F. Di Virglio, M. Beltrame, R. Y. Tsien, and T. Pozzan. 1985. Cytosolic Ca^{2+} homeostasis in Erlich and Yoshida carcinomas. A new, membrane permeant chelator of heavy metals reveals that these ascites tumor cell lines have normal cytosolic free calcium. *J. Biol. Chem.* 260: 2719–2727.

Bancel, F., J.-M. Salmon, J. Vigo, T. Vo-Dinh, and P. Viallet. 1992. Investigation of noncalcium interactions of Fura-2 by classical and synchronous fluorescence spectroscopy. *Anal. Biochem.* 204:231–238.

Baylor, D. A., T. D. Lamb, and K.-W. Yau. 1979. The membrane current of single rod outer segments. *J. Physiol.* 288:589–611.

Baylor, D. A., and B. J. Nunn. 1986. Electrical properties of the light-sensitive conductance of rods of the salamander *Ambystoma tigrinum*. *J. Physiol.* 371:115–145.

Blatter, L. A., and W. G. Wier. 1990. Intracellular diffusion, binding, and compartmentalization of the fluorescent calcium indicators indo-1 and fura-2. *Biophys. J.* 58:1491–1499.

Bownds, M. D. 1980. Biochemical steps in visual transduction: roles for nucleotides and calcium ions. *Photochem. Photobiol.* 32:487–490.

Capovilla, M., L. Cervetto, and V. Torre. 1983. The effect of phosphodiesterase inhibitors on the electrical activity of toad rods. *J. Physiol.* 343: 277–294.

Cervetto, L., L. Lagnado, R. J. Perry, D. W. Robinson, and P. A. McNaughton. 1989. Extrusion of calcium from rod outer segments is driven by both sodium and potassium gradients. *Nature.* 337:740–743.

Cervetto, L., and P. A. McNaughton. 1986. The effects of phosphodiesterase inhibitors and lanthanum ions on the light-sensitive current of toad retinal rods. *J. Physiol.* 370:91–109.

Chiancone, E., E. Thulin, A. Boffi, S. Forsén, and M. Brunori. 1986. Evidence for the interaction between the calcium indicator 1,2-bis(*o*-aminophenoxy)ethane-N,N,N′,N′-tetraacetic acid and calcium-binding proteins. *J. Biol. Chem.* 261:16306–16308.

Cobbold, R. S. C. 1974. Transducers for Biomedical Applications: Principles and Applications. John Wiley & Sons, New York. 486 pp.

Dizhoor, A. M., S. Ray, S. Kumar, G. Niemi, M. Spencer, D. Brolley, K. Walsh, P. P. Philipov, J. B. Hurley, and L. Stryer. 1991. Recoverin: a calcium sensitive activator of retinal rod guanylate cyclase. *Science.* 251: 915–918.

Fain, G. L., B. L. Bastian, and H. M. Gerschenfeld. 1978. Contribution of a caesium-sensitive conductance increase to the rod photoresponse. *Nature.* 272:467–469.

Furakawa, T., and I. Hanawa. 1955. Effects of some common cations on electroretinogram of the toad. *Japan. J. Physiol.* 5:289–300.

Gray-Keller, M. P., and P. B. Detwiler. 1994. Intracellular calcium measurements in isolated rod outer segments. *Invest. Opthalmol. & Visual Sci.* 35:1486*a*. (Abstr.)

Groden, D. L., Z. Guan, and B. T. Stokes. 1991. Determination of Fura-2 dissociation constants following adjustment of the apparent Ca-EGTA association constant for temperature and ionic strength. *Cell Calcium.* 12:279–287.

Grynkiewicz, G., M. Poenie, and R. Y. Tsien. 1985. A new generation of Ca^{2+} indicators with greatly improved fluorescence properties. *J. Biol. Chem.* 260:3440–3450.

Hárosi, F. I. 1975. Absorption spectra and linear dichroism of some amphibian photoreceptors. *J. Gen. Physiol.* 66:357–382.

Hodgkin, A. L., P. A. McNaughton, and B. J. Nunn. 1985. The ionic selectivity and calcium dependence of the light-sensitive pathway in toad rods. *J. Physiol.* 358:447–468.

Hodgkin, A. L., P. A. McNaughton, and B. J. Nunn. 1987. Measurement of sodium-calcium exchange in salamander rods. *J. Physiol.* 391:347–370.

Hove-Madsen, L., and D. M. Bers. 1992. Indo-1 binding to protein in permeabilized ventricular myocytes alters its spectral and calcium binding properties. *Biophys. J* 63:89–97.

Kawamura, S. 1993. Rhodopsin phosphorylation as a mechanism of cyclic GMP phosphodiesterase regulation by S-modulin. *Nature.* 362: 855–857.

Kawamura, S., and M. Murakami. 1991. Calcium-dependent regulation of cyclic GMP phosphodiesterase by a protein from frog retinal rods. *Nature.* 349:420–423.

Koch, K.-W., and L. Stryer. 1988. Highly cooperative feedback control of retinal rod guanylate cyclase by calcium ions. *Nature.* 334:64–66.

Konishi, M., A. Olson, S. Hollingworth, and S. M. Baylor. 1988. Myoplasmic binding of Fura-2 investigated by steady-state fluorescence and absorbance measurements. *Biophys. J.* 54:1089–1104.

Korenbrot, J. I., and D. L. Miller. 1989. Cytoplasmic free calcium concentration in dark-adapted retinal rod outer segments. *Vision. Res.* 29: 939–948.

Lagnado, L., L. Cervetto, and P. A. McNaughton. 1988. Ion transport by the Na-Ca exchange in isolated rod outer segments. *Proc. Natl. Acad. Sci. USA.* 85:4548–4552.

Lagnado, L., L. Cervetto, and P. A. McNaughton. 1992. Calcium homeostasis in the outer segments of retinal rods from the tiger salamander. *J. Physiol.* 455:111–142.

Lagnado, L., and D. A. Baylor. 1994. Calcium controls light-triggered formation of catalytically active rhodopsin. *Nature.* 367:273–237.

Lolley, R. N., and E. Racz. 1982. Calcium modulation of cyclic GMP synthesis in rat visual cells. *Vision Res.* 22:1481–1486.

Martell, A. E., and R. M. Smith. 1974. Critical Stability Constants, Vol. 1. Plenum Press, New York.

Matthews, G. 1983. Physiological characteristics of single green rod photoreceptors from toad retina. *J. Physiol.* 342:347–359.

Matthews, H. R., R. L. W. Murphy, G. L. Fain, and T. D. Lamb. 1988. Photoreceptor light adaptation is mediated by cytoplasmic calcium concentration. *Nature.* 334:67–69.

McCarthy, S. T. 1993. Calcium, cyclic GMP metabolism and light adaptation in rods of the bullfrog. Ph.D. Thesis. University of California, Berkeley and San Francisco.

McNaughton, P. A., L. Cervetto, and B. J. Nunn. 1986. Measurement of the intracellular free calcium concentration in salamander rods. *Nature.* 322: 261–263.

Miller, D. L., and J. I. Korenbrot. 1987. Kinetics of light-dependent Ca fluxes across the plasma membrane of rod outer segments. *J. Gen. Physiol.* 90:397–425.

Nakatani, K., and K.-W. Yau. 1988. Calcium and light adaptation in retinal rods and cones. *Nature.* 334:69–71.

Negulescu, P. A., and T. E. Machen. 1990. Intracellular ion activities and membrane transport in parietal cells measured with fluorescent dyes. *Methods Enzymol.* 192:38–81.

Pepe, I. M., A. Boero, L. Vergani, I. Panfoli, and C. Cugnoli. 1986. Effect of light and calcium on cyclic GMP synthesis in rod outer segments of toad retina. *Biochim. Biophys. Acta.* 889:271–276.

Pepperberg, D. R., J. Jin, and G. J. Jones. 1994. Modulation of transduction gain in light adaptation of retinal rods. *Visual Neurosci.* 11:53–62.

Poenie, M. 1990. Alteration of intracellular Fura-2 fluorescence by viscosity: a simple correction. *Cell Calcium.* 11:85–91.

Pugh, E., and J. Altman. 1988. A role for calcium in adaptation. News and Views. *Nature.* 334:16–17.

Ratto, G. M., R. Payne, W. G. Owen, and R. Y. Tsien. 1988. The concentration of cytosolic free calcium in vertebrate rod outer segments measured with Fura-2. *J. Neurosci.* 8:3240–3246.

Robinson, P. R., S. Kawamura, B. Abramson, and M. D. Bownds. 1980. Control of the cyclic GMP phosphodiesterase of frog photoreceptors membranes. *J. Gen. Physiol.* 76:631–645.

Roe, M. W., J. J. LeMasters, and B. Herman. 1990. Assessment of Fura-2 for measurements of cytosolic free calcium. *Cell Calcium* 11:63–73.

Rosenkranz, J. 1972. New aspects of the ultrastructure of frog rod outer segments. *Int. Rev. Cytol.* 50:24–158.

Schnetkamp, P. P. M. 1991. Optical measurements of Na-Ca-K exchange currents in intact outer segments isolated from bovine retinal rods. *J. Gen. Physiol.* 98:555–573.

Schnetkamp, P. P. M., D. K. Basu, X.-B. Li, and R. T. Szerencsei. 1991. Regulation of intracellular free Ca^{2+} concentration in the outer segments

of bovine retinal rods by Na-Ca-K exchange measured with Fluo-3. *J. Biol. Chem.* 266:22983–22990.

Schnetkamp, P. P. M., D. K. Basu, and R. T. Szerencsei. Na^+-Ca^{2+} exchange in bovine rod outer segments requires, and transports K^+. *Am. J. Physiol.* 337:740–743.

Schnetkamp, P. P. M., and R. T. Szerencsei. 1993. Intracellular Ca^{2+} sequestration and release in intact bovine retinal rod outer segments. *J. Biol. Chem.* 268:12449–12457.

Schröder, W. H., and G. L. Fain. 1984. Light-dependent calcium release from photoreceptors measured by laser micro-mass analysis. *Nature*. 309: 268–270.

Somlyo, A. P., and B. Walz. 1985. Elemental distribution in *Rana pipiens* retinal rods: quantitative electron probe analysis. *J. Physiol.* 358: 183–195.

Szuts, E. Z., and R. A. Cone. 1977. Calcium content of frog rod outer segments and discs. *Biochim. Biophys. Acta*. 486:194–208.

Torre, V., H. R. Matthews, and T. D. Lamb. 1986. Role of calcium in regulating the cyclic GMP cascade of phototransduction in retinal rods. *Proc. Natl. Acad. Sci. USA*. 83:7109–7113.

Tsien, R. Y., and A. T. Harootunian. 1990. Practical design criteria for a dynamic ratio imaging system. *Cell Calcium*. 11:93–109.

Tsien, R. Y., and T. J. Rink. 1980. Neutral carrier ion-selective microelectrodes for measurement of intracellular free calcium. *Biochim. Biophys. Acta*. 599:623–638.

Wagner, R., R. Nicholas, and R. Uhl. 1989. Calcium regulates the rate of rhodopsin disactivation and the primary amplification step in visual transduction. *FEBS Lett.* 242:249–254.

Williams, D. A., and F. S. Fay. 1990. Intracellular calibration of the fluorescent calcium indicator Fura-2. *Cell Calcium*. 11:75–83.

Uto, A., H. Arai, and Y. Ogawa. 1991. Reassessment of Fura-2 and the ratio method for determination of intracellular Ca^{2+} concentrations. *Cell Calcium*. 12:29–37.

Yau, K.-W., and K. Nakatani. 1985. Light-induced reduction of cytoplasmic free calcium in retinal rod outer segment. *Nature*. 313:579–582.

Younger, J. P. 1991. Calcium regulation of the light response of vertebrate photoreceptors. Ph.D. Thesis. University of California, Berkeley.

Younger, J. P., S. T. McCarthy, and W. G. Owen. 1992. Modulation of cytosolic free calcium and changes in sensitivity and circulating current occur over the same range of steady-state adapting lights in rod photoreceptors. *Invest. Opthalmol. & Visual Sci.* 33:1104*a*. (Abstr.)